EFFECT OF FLOATING $p - n$ JUNCTIONS ON THE EFFICIENCY OF SILICON BACK SIDE CONTACT SOLAR CELLS

A.P. GORBAN, V.P. KOSTYLYOV, A.V. SACHENKO, O.A. SERBA, I.O. SOKOLOVSKYI, V.V. CHERNENKO

V.E. Lashkaryov Institute of Semiconductor Physics, Nat. Acad. of Sci. of Ukraine
(41, Nauky Ave., Kyiv 03028, Ukraine)

PACS 71.55.Cn, 72.20.Jv

Characteristics of silicon back side contact solar cells are investigated theoretically and experimentally at low illumination levels in the presence of a floating $p^+ - n$ junction on the front surface. It is established that, under these conditions, the short-circuit current, open-circuit voltage, and internal quantum efficiency of photocurrent can significantly decrease due to the influence of recombination in the near-surface space charge region. The interval of irradiances, in which these reductions are essential enough, is determined. In particular, it is shown that the interval of light intensities corresponding to a decrease of the open-circuit voltage V_{OC} is significantly wider than that corresponding to a reduction of the short-circuit current J_{SC}. The experimental results agree with those of calculations. The obtained results allow us to conclude that the floating $p^+ - n$ junctions on the front surface of silicon back side contact solar cells are appropriate for the use only at significantly large levels of illumination intensities (≥ 1000 W/m^2).

1. Introduction

Commercial samples of up-to-date silicon back side contact (BSC) solar cells (SC) with n-type base, as well as modules produced on their basis, are characterized by the highest efficiency of photoelectrical energy conversion η achieved till now that amounts to 22.4% for cells and 20.1 % for modules [1]. As a rule, the thickness of a quasineutral base in such BSC SCs is much lower than the diffusion length of minority carriers, whereas the effective surface recombination velocity S_{ef} on the front (nonmetallized) surface referred to the inner boundary of the near-surface space charge region (SCR) is minimized to the level that practically does not influence the value of η.

A detailed theoretical analysis of the factors that determine the effective surface recombination velocity S_{ef} in silicon-based solar cells, where nonequilibrium electron-hole pairs recombine mainly via surface recombination centers, is performed in [2]. With the use of the self-consistent approach, it was demonstrated that, depending on the charge state of the near-surface SCR and the concentration of doping agents in the emitter and base region, the effective surface recombination velocity S_{ef} can either grow or fall with increase in the concentration Δn of nonequilibrium charge carriers in a quasineutral volume. Moreover, at sufficiently high injection levels, the velocity S_{ef} saturates and is determined solely by parameters of surface recombination centers.

As is known, the most effective way to eliminate surface recombination losses in BSC SCs is the generation of isotype $n^+ - n$ or $p^+ - p$ junctions on their front surface that limit the supply of nonequilibrium minority carriers to surface recombination centers [3,4]. In the presence of such junctions, the effective surface recombination velocity S_{ef} is minimized due to a decrease of the true recombination velocity of nonequilibrium charge carriers via surface recombination centers [2], though, at high doping levels of the surface layer, the velocity S_{ef} can rise due to an increase of the velocity of Auger recombination in this layer [3]

A number of works [5, 6] used another way of minimization of the negative influence of surface recombination losses on the efficiency of BSC SCs η, namely the formation of floating $p^+ - n$ or $n^+ - p$ junctions on their front surface that limited the supply of nonequilibrium majority carriers to surface recombination centers. However, the experimental researches performed in [6] demonstrated that, though the formation of a floating $n^+ - p$ junction really resulted in an increase of the efficiency of BSC SCs η under the standard spectral conditions AM1.5 at the irradiance $P_L = 1000$ W/m^2, a considerable (tens-fold) rise of the effective surface recombination velocity S_{ef} was simultaneously observed. Such an anomalous behavior of the dependence $\eta(S_{ef})$ could not be logically explained in the framework of the physical model of BSC SCs proposed in [6].

In the given work, it is shown that, in the presence of a floating $p^+ - n$ or $n^+ - p$ junction on the front (illuminated) surface, the recombination in the SCR of the floating junction becomes the dominant recombina-

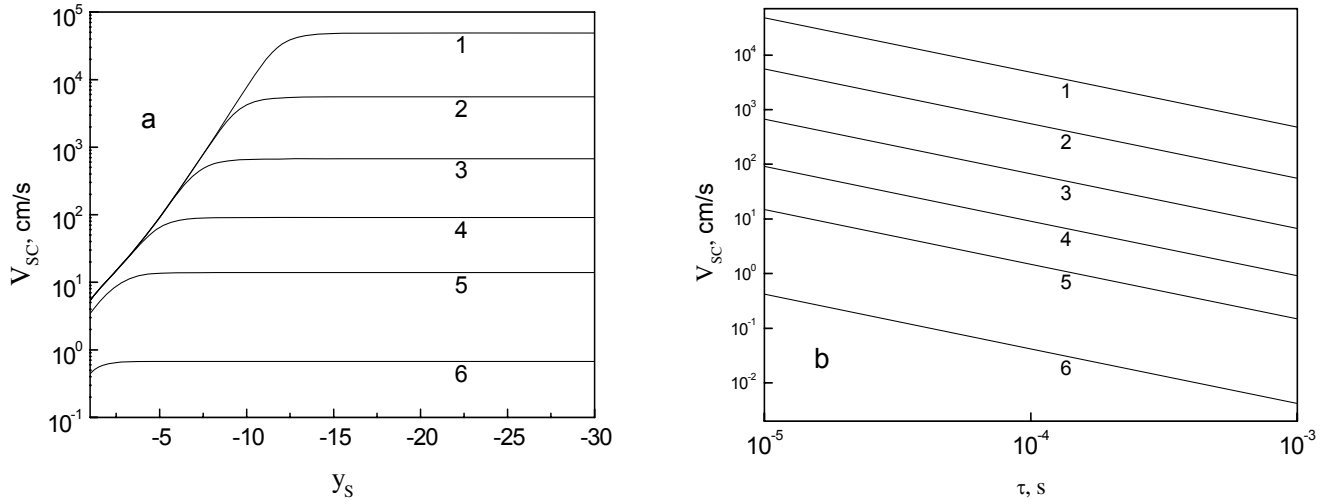

Fig. 1. Effective SCR recombination velocity $V_{\rm SC}$ as a function of the dimensionless energy band bending near the illuminated surface y_s (*a*) and the bulk lifetime τ (*b*); $n_0 = 10^{15}$ cm^{-3}, $p_0 = 10^5$ cm^{-3}, $\Delta p = 0$ (*1*), 10^7 (*2*), 10^9 (*3*), 10^{11} (*4*), 10^{13} (*5*), and 10^{15} cm^{-3} (*6*)

tion mechanism in BSC SCs at small light intensities. It is known that, in silicon solar cells of the common type, this recombination mechanism practically does not influence the magnitude of the short-circuit current, because the photogeneration and the collection of nonequilibrium electron-hole pairs take place mainly within the SCR of the collector junction, where nonequilibrium electrons and holes are separated by a strong electric field without recombination. But, in BSC SCs where the quasineutral base separates the regions of photogeneration and collection of nonequilibrium electron-holes pairs, the recombination in the SCR of a floating $p^+ - n$ or $n^+ - p$ junction must essentially influence both the short-circuit current and the form of its spectral dependence measured at low light fluxes with the use of a monochromator.

2. Theoretical Analysis of the Mechanisms of Influence of SCR Recombination on *Photoenergy* Parameters of BSC SCs

In order to calculate the effective SCR recombination velocity and its dependence on the dimensionless potential on the illuminated surface of a BSC SC y_s, the bulk recombination lifetime τ, and the excess concentration of pairs at the interface of the SCR and the quasineutral region Δp, we use the model of one deep recombination center located close to the middle of the energy gap. It will be considered that the recombination in the SCR takes place via the same recombination center responsible for the bulk recombination. For an n-type semiconductor, we can write

$$V_{\rm SC}(\Delta p) = \frac{L_{\rm D}}{\tau}\int\limits_{y_s}^{0}(n_0)/\left(\left[n_0 e^y + \frac{C_p}{C_n}\left(p_0+\Delta p\right)e^{-y}\right]\times\right.$$

$$\left.\times\sqrt{-y+(e^y-1)+\frac{(p_0+\Delta p)}{n_0}e^{-y}}\right)dy, \qquad (1)$$

where $V_{\rm SC}$ denotes the effective SCR recombination velocity, $L_{\rm D} = (\varepsilon_0\varepsilon_s kT/2q^2n_0)^{0.5}$ is the Debye length, τ is the bulk recombination time, n_0 and p_0 stand for the equilibrium concentrations of electrons and holes, respectively, while C_n and C_p are their capture efficiencies.

Figure 1,*a* shows the theoretically calculated effective SCR recombination velocities $V_{\rm SC}$ as functions of the dimensionless potential on the illuminated BSC SC surface y_s in the case where n_0=10^{15} cm^{-3}, $p_0 = 10^5$ cm^{-3}, $\tau = 10^{-5}$ s, and $C_n = C_p$. The curves are plotted for different excess concentrations of holes Δp at the boundary of the SCR and the quasineutral region. One can see that, with increase in the band bending y_s, the value of $V_{\rm SC}$ rises, being saturated at $-y_s > (1/2)\ln(n_0/(p_0+\Delta p))$. An increase in Δp results in a fall of the velocity $V_{\rm SC}$ in the saturation region and the widening of the latter. The figure also demonstrates that, at $\Delta p \approx 10^{15}$ cm^{-3} (which is typical of the AM0 or AM1.5 conditions), the value of $V_{\rm SC}$ decreases by five orders of magnitude as compared with the case where no photogeneration is present. In the case of BSC SCs, it is

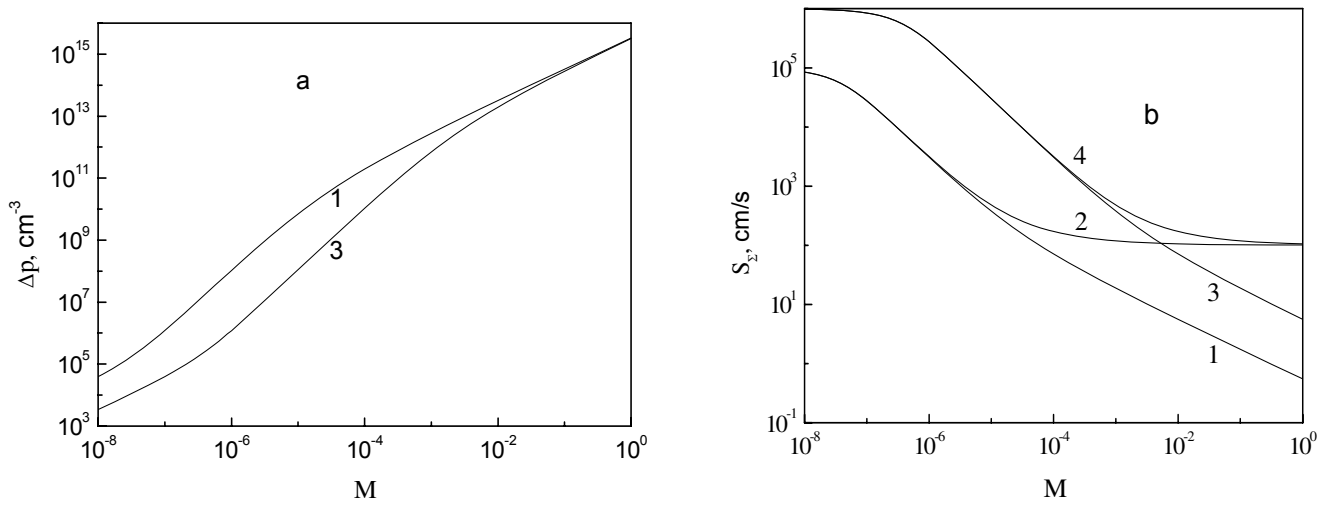

Fig. 2. Dependences of Δp (a) and the total effective surface recombination velocity $S_\Sigma = (S_{\rm ef} + V_{\rm SC}(M) + d/2\tau)$ (b) on the concentration degree of solar radiation M; $n_0 = 10^{15}$ cm^{-3}, $p_0 = 10^5$ cm^{-3}, $S_{\rm ef} + d/2\tau = 10^2$ cm/s, $V_{\rm SC}(0) = 10^5$ (*1, 2*) and 10^6 (*3, 4*) cm/s

important to minimize the summary velocity of recombination via surface centers and SCR recombination to the level ≤ 1 cm/s, at which surface recombination losses become an order of magnitude lower than bulk ones.

The velocities $V_{\rm SC}$ as functions of the bulk recombination lifetime τ calculated for the case $y_s = -15$ are presented in Fig. 1,*b*. One can see that, at $\Delta p = 10^{15}$ cm^{-3} and $\tau \geq 10^{-5}$ s, the SCR recombination can be neglected really as compared with the bulk one, because the velocity of the former approximates 1 cm/s at $\tau = 10^{-5}$ s. Thus, the SCR recombination can affect the short-circuit current in BSC SCs and its spectral dependences only under the conditions where the optical generation intensity I becomes much lower than its value under the usual AM0 conditions $I_{\rm AM0}$ corresponding to the value of 3.37×10^{17} quanta/cm^{2}s in the case of silicon.

Let us perform a self-consistent analysis of the dependence of the excess hole concentration Δp on $I = MI_{\rm AM0}$, where M is the numerical coefficient characterizing the attenuation degree of the solar radiation flux that can vary in the interval between 0 and 1. In the region of small I at $\Delta p \leq n_0$, both surface and bulk recombinations do not any more depend on the optical generation intensity. That is why the equation of generation-recombination balance in BSC SCs can be presented in the form

$$\left(S_{\rm ef} + V_{\rm SC}(\Delta p) + \frac{d}{2\tau}\right)\Delta p = MI_{\rm AM0}. \qquad (2)$$

The first term in the parentheses of expression (2) describes the contribution made to the total recombination flux by recombination via surface centers $S_{\rm ef}$, the second one — by the SCR recombination, and the third — by the bulk one.

Figure 2,*a* presents the dependences $\Delta p(M)$, while Fig. 2,*b* shows the dependences $V_{\rm SC}(M)$ (curves *1, 3*) and $S_\Sigma M = S_{\rm ef} + V_{\rm SC}(M) + d/2\tau$ (curves *2, 4*) resulting from the self-consistent solution of Eqs. (1) and (2) at two values of $V_{\rm SC}(0)$. One can see from Fig. 2,*a* that the dependences $\Delta p(M)$ consist of three regions corresponding to different recombination mechanisms — linear at $\Delta p < p_0$, ultralinear at $\Delta p > p_0$ and $V_{\rm SC} > S_{\rm ef} + d/2\tau$, and one more linear at $\Delta p > p_0$ and $V_{\rm SC} < S_{\rm ef} + d/2\tau$. It is worth expecting that the short-circuit current of BSC SCs in the ultralinear region of the dependence $\Delta p(M)$ will also increase ultralinearly. Moreover, the value of M corresponding to a change of the dominant recombination mechanism depends on the initial value of the SCR recombination velocity $V_{\rm SC}(0)$ (Fig. 2,*b*).

The internal quantum efficiency Q in silicon BSC SCs in the case of monochromatic illumination can be found from the solution of the diffusion equation with the following boundary conditions:

$$j(x = 0) = -(S_{\rm ef} + V_{\rm SC}(M))\Delta p(x = 0), \qquad (3)$$

$$\Delta p(x = d) = 0. \qquad (4)$$

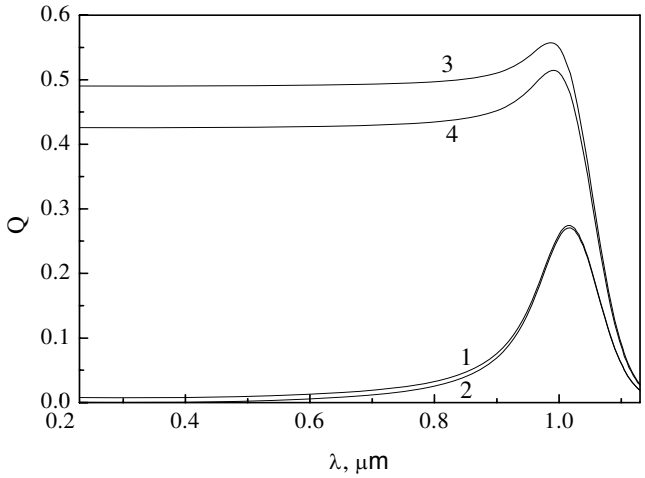

Fig. 3. Spectral dependences of the internal quantum efficiency in the BSC SC at $M = 10^{-7}$ (*1, 2*) and $M = 10^{-2}$ (*3, 4*); $n_0 = 10^{15}$ cm^{-3}, $p_0 = 10^5$ cm^{-3}, $S_{\text{ef}} + d/2\tau = 10^2$ cm/s, $L = 4 \times 10^{-2}$ cm, $d = 4 \times 10^{-2}$ cm; $V_{\text{SC}}(0) = 10^5$ (*1, 3*) and 10^6 (*2, 4*) cm/s

As a result, one obtains the internal quantum efficiency Q in the form

$$Q = \frac{\alpha L}{1-\alpha^2 L^2} \times$$

$$\times \left\{ \frac{-\left[\frac{S^* L}{D}\left(1 - e^{-\alpha d - d/L}\right) + \alpha L + e^{-\alpha d - d/L}\right]}{\cosh\left(\frac{d}{L}\right) + \frac{S^* L}{D}\sinh\left(\frac{d}{L}\right)} + \right.$$

$$\left. + (1 + \alpha L)\, e^{-\alpha d} \right\}, \qquad (5)$$

where $L = (D\tau)^{1/2}$ stands for the diffusion length of holes, D is their diffusion coefficient, α is the light absorption coefficient in silicon at $T = 300$ K [7], and $S^* = S_{\text{ef}} + V_{\text{SC}}(M)$.

The spectral dependences of the internal quantum efficiency Q in BSC SCs in two cases where $M = 10^{-7}$ (curves *1, 2*) and $M = 10^{-2}$ (curves *3, 4*) are plotted in Fig. 3. One can see that the shapes of these curves considerably differ. Moreover, curves *1* and *2* in Fig. 3 are typical of solar cells with a high effective velocity of surface recombination S_{ef}. In this case, the dominant contribution to S^* is made by the SCR recombination (see Fig. 2,*b*). In the other case shown in curves *3, 4*, the spectral dependences of the internal quantum efficiency are typical of solar cells with comparatively low effective velocities of surface recombination S^*. This situation corresponds to relatively high irradiances in Fig. 2,*b* ($M \geq 10^{-2}$), where recombination mainly takes place via recombination centers.

Denoting the spectrum-averaged coefficient of light reflection from the BSC SC surface by r_s and multiplying (5) by $(1-r_s)I$, we obtain the spectral dependence of the short-circuit current at the optical generation intensity I. In this case, the density of the short-circuit current of a unit square silicon BSC SC (mA/cm^2) as a function of M for the AM0 spectral conditions can be obtained from the expression

$$J_{\text{SC}}(M) = (1 - r_s) \int_0^{1.13} \frac{654.7 MQ}{\lambda^4 \left[\exp\left(\frac{2.5}{\lambda}\right) - 1\right]} d\lambda, \qquad (6)$$

where the illumination wavelength λ is measured in micrometers.

Expression (6) was derived in the assumption that the solar radiation spectrum under the AM0 conditions represents the spectrum of a black body with a temperature of 5800 K.

Figure 4,*a* presents the short-circuit current density J_{SC} as a function of M normalized to the current density at $M = 1$. One can see that the largest deviations from the linearity (curve *1*) are observed for M lying in the interval between 10^{-8} and 10^{-5} at $V_{\text{SC}}(M = 0) = 10^6$ cm/s (curve *4*) and somewhat smaller ones — at $V_{\text{SC}}(M = 0) = 10^5$ cm/s (curve *3*). If $V_{\text{SC}}(M = 0) = 10^3$ cm/s (which corresponds to $\tau \approx 10^{-3}$ s), then the dependence $J_{\text{SC}}(M)$ appears to be practically linear at $M > 10^{-5}$ (curve *2*). It is essential that, at the parameters used in our calculations, the dependences $J_{\text{SC}}(M)$ are linear at $M \geq 10^{-2}$.

It is worth noting that the SCR recombination characterized by the ideality factor of VACs $\beta = 2$ can considerably influence the open-circuit voltage V_{OC} both in common solar cells and in BSC SCs. In the general case where one takes both the recombination and diffusion mechanisms of current passage into account, the voltage V_{OC} is usually calculated with the use of the expression

$$J_{\text{ds}}\left(\exp\left(\frac{qV_{\text{OC}}}{kT}\right) - 1\right) + J_{\text{rs}}\left(\exp\left(\frac{qV_{\text{OC}}}{2kT}\right) - 1\right) =$$

$$= qMI_{\text{AM0}}. \qquad (7)$$

The effective SCR recombination velocity and the recombination saturation current density are connected by the following relation

$$V_{\text{SC}}(\Delta p) = \frac{J_{\text{rs}}}{q}\left(\left(\frac{\Delta p}{p_0} + 1\right)^{1/2} - 1\right)\Delta p^{-1}, \qquad (8)$$

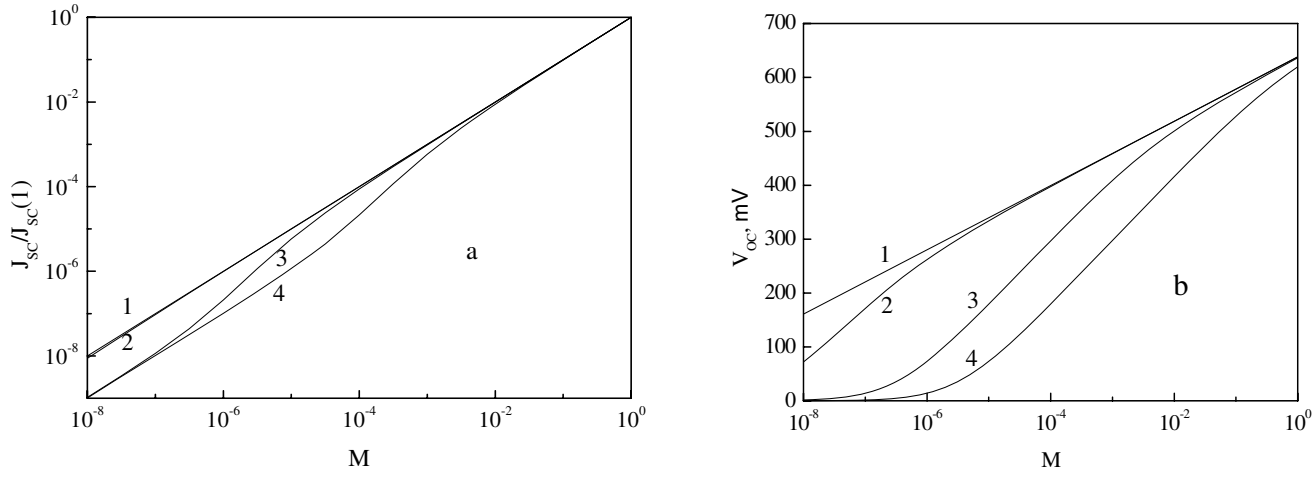

Fig. 4. Dependences of $J_{\rm SC}$ (*a*) and $V_{\rm OC}$ (*b*) on the concentration degree M. The set of parameters is the same as in Fig. 3. $V_{\rm SC}(0) = 0$ (*1*), 10^3 (*2*), 10^5 (*3*), and 10^6 (*4*) cm/s (*a*); $J_{\rm ds} = 2 \times 10^{-13}$ A/cm^2, $J_{\rm rs} = 0$ (*1*), 3.2×10^{-11} (*2*), 3.2×10^{-9} (*3*), and 3.2×10^{-8} (*4*) A/cm^2 (*b*)

where q is the electron charge, k is the Boltzmann constant, T is the temperature, while $J_{\rm ds}$ and $J_{\rm rs}$ are the densities of diffusion and recombination saturation currents, respectively. Expression (8) allows one to derive the relation between $V_{\rm SC}(\Delta p = 0)$ and $J_{\rm rs}$. For example, at $V_{\rm SC}(\Delta p = 0) = 10^6$ cm/s, one obtains $J_{\rm rs} = 3.2 \times 10^{-8}$ A/cm^2, whereas at $V_{\rm SC}(\Delta p = 0) = 10^5$ cm/s, $J_{\rm rs}$ amounts to 3.2×10^{-9} A/cm^2.

The dependences $V_{\rm OC}(M)$ calculated with the use of expression (7) are plotted in Fig. 4,*b*. Our calculations were carried out for the diffusion saturation current density $J_{\rm ds} = 2 \times 10^{-13}$ A/cm^2 corresponding to the bulk recombination velocity approximating 10 cm/s at $\tau = 10^{-3}$ s. Curve *1* describes the case where SCR recombination is absent. Curve *2* is plotted with the use of the value $J_{\rm rs} = 3.2 \times 10^{-11}$ A/cm^2, which corresponds to $V_{\rm SC}(\Delta p = 0) = 10^3$ cm/s. Curve *3* is plotted for the current density $J_{\rm rs}$= 3.2×10^{-9} A/cm^2, while curve *4* – for 3.2×10^{-8} A/cm^2. One can see from Fig. 4,*b* that an increase of the SCR recombination velocity $V_{\rm SC}(\Delta p = 0)$ results in a decrease of the open-circuit voltage $V_{\rm OC}$ of the BSC SC at low light intensities, whereas the effect of the SCR recombination on the voltage $V_{\rm OC}$ appears at larger M. Comparing Figs. 4,*a* and 4,*b*, one can also conclude that the SCR recombination influences the open-circuit voltage stronger than the short-circuit current. For example, at $V_{\rm SC}(\Delta p = 0) = 10^3$ cm/s, the SCR recombination practically has no effect on the short-circuit current at $M > 10^{-5}$, though it influences the open-circuit voltage even at $M \approx 1$.

In order to estimate the effect of SCR recombination on the efficiency of photoelectrical energy conversion in BSC SCs, we consider the ratio of the products of the short-circuit current by the open-circuit voltage in the presence and in the absence of SCR recombination. Denoting this ratio by K, we write the expression for it in the form

$$K(M) = \frac{J_{\rm SC} V_{\rm OC}}{J^0_{\rm SC} V^0_{\rm OC}}, \tag{9}$$

where the index "0" means that the SCR recombination is absent.

Figure 5 shows the dependences $K(M)$ calculated for different values of the parameter $V_{\rm SC}(\Delta p = 0)$. One can see that, at sufficiently low levels of irradiance, the SCR recombination considerably influences the efficiency of photoelectrical energy conversion if $V_{\rm SC}(\Delta p = 0) \geq 10^4$ cm/s.

Thus, the results of the theoretical analysis performed in the given work allow us to conclude that the use of floating $p^+ - n$ or $n^+ - p$ junctions as antirecombination barriers on the front (illuminated) surface of silicon back side contact solar cells can represent an effective way to decrease surface recombination losses only under the condition of their use at high irradiances of the surface ($P_L \geq 1000$ W/m^2). Otherwise, their use is unreasonable, because it can lead to an essential decrease of the efficiency of photoelectrical energy conversion.

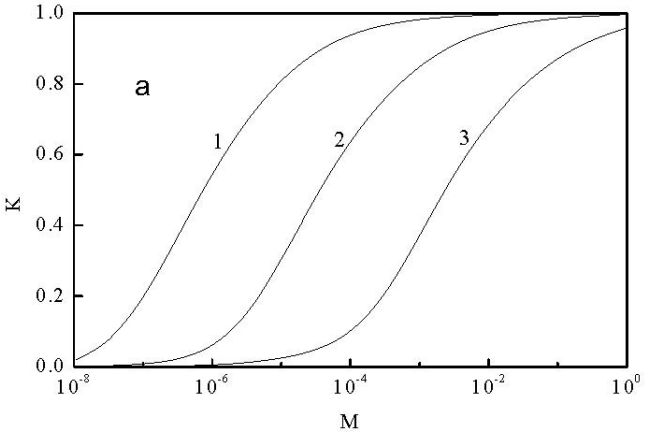

Fig. 5. Dependences $K(M)$ plotted with the use of the same parameters as in Fig. 3. $V_{\rm SC}(0) = 10^4$ (*1*), 10^5 (*2*), and 10^6 (*3*) cm/s

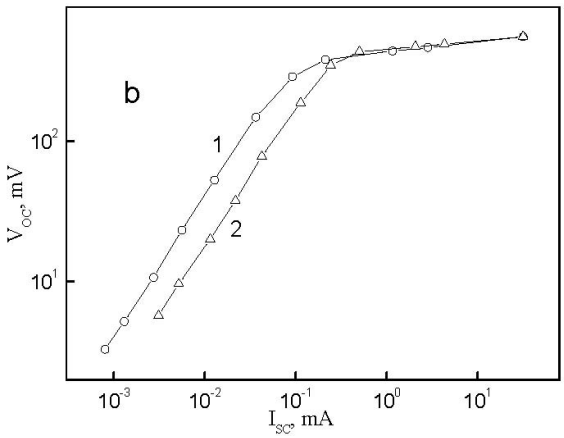

Fig. 6. Dependences of the open-circuit voltage $V_{\rm OC}$ on the short-circuit current $I_{\rm SC}$ for the BSC SC samples with an isotype (curve *1*) and floating (curve *2*) junctions on the front surface

3. Experimental Results and Their Discussion

Comparative experimental investigations of antirecombination properties of isotype and floating junctions were performed for BSC SC samples with the n−-type base produced on the basis of KBE-2 zone-melting silicon plates with a resistivity approximating 2 Ohm×cm. These BSC SCs were produced using the same technology except for high-temperature operations related to the creation of phosphorus-doped isotype $n^+ - n$ or boron-doped floating $p^+ - n$ junctions on the front surface. In order to reduce optical losses, we formed a 110-nm SiO_2 film on the front surface of the doped layers with the help of thermal oxidation at a temperature of 900 °C. Aluminum ohmic contacts on the back surface of the BSC SCs were created by means of the vacuum deposition of aluminum on the surface of doped n^+ and p^+ regions through the windows in the SiO_2 film created by photolithography techniques. The resistivity of the contacts was reduced by means of the heating of the BSC SC samples in vacuum at a temperature of 400 °C after photolithography.

The phototechnical and spectral characteristics of the BSC SCs were measured with the help of a control-measuring equipment of the Center for testing photoconverters and photoelectric batteries of the V.E. Lashkaryov Institute of Semiconductor Physics of the National Academy of Sciences of Ukraine certified by the State Committee of Ukraine for Technical Regulation and Consumer Policy. In the course of measuring the spectral dependences of the short-circuit current, a constant level of the light flux power was maintained automatically, whereas phototechnical parameters of BSC SCs (short-circuit current, open-circuit voltage) were measured under the AM1.5 spectral conditions at solar illumination. The irradiance of the BSC SC surface was changed in a wide range with the help of neutral filters.

Figure 6 presents the experimental dependences of the open-circuit voltage $V_{\rm OC}$ on the short-circuit current $I_{\rm SC}$ obtained for the BSC SCs with an isotype $n^+ - n$ (curve *1*) and floating $p^+ - n$ (curve *2*) junctions on the front surface at different intensities of the solar illumination. As a rule, the form of these dependences is determined by the saturation current density and the ideality factor of collector $p^+ - n$ junctions located (in this case) on the BSC SC back surface. One can see from the figure that, at sufficiently high levels of the irradiance $P_L(M \geq 10^{-2})$, these dependences coincide, while they are parallel to each other at low ones. Moreover, one observes two regions in the dependences $V_{\rm OC}(I_{\rm SC})$ that have different slopes and correspond to the VAC ideality factors $\beta \approx 1$ at high levels of the irradiance P_L of the front BSC SC surface and $\beta \approx 2$ – in the region of low P_L. As nonequilibrium electron-hole pairs diffuse to the collector junction from the front surface in the case of BSC SCs, this means (according to formula (2)) that surface recombination losses in the collector $p^+ - n$ junction on the back surface at high $V_{\rm OC}$ are practically absent, whereas the main recombination mechanism is the bulk recombination at high injection levels. At the same time, the divergence of the dependences $V_{\rm OC}(I_{\rm SC})$ at low $V_{\rm OC}$ is explained according to (7) by the fact that the values of $J_{\rm rs}$ in BSC SCs with a floating $p^+ - n$

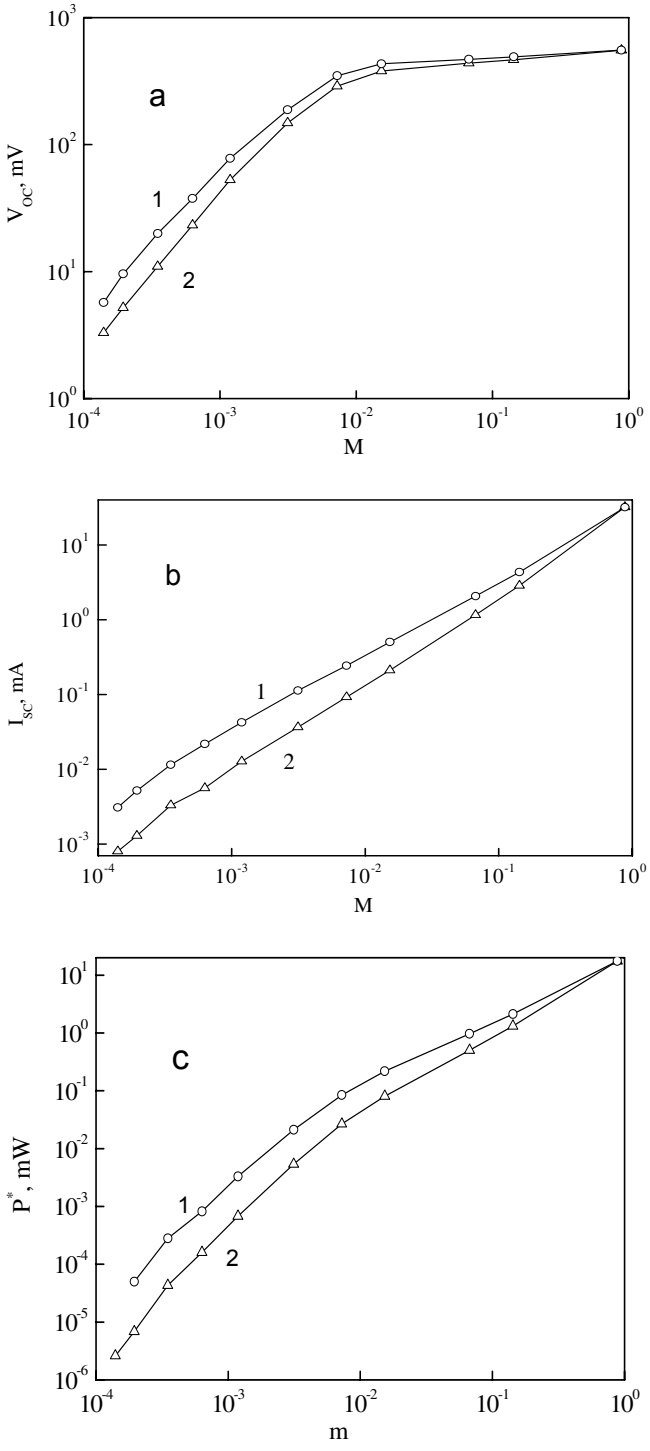

Fig. 7. Dependences $V_{\rm OC}$ (*a*), $I_{\rm SC}$ (*b*), and $P^* = I_{\rm SC} \times V_{\rm OC}$ (*c*) on the concentration degree M of ground solar radiation under the AM1.5 spectral conditions ($P_L = 1000$ W/m^2) obtained for the BSC SC samples with isotype $n^+ - n$ (curves *1*) and floating $p^+ - n$ (curves *2*) junctions on the front surface

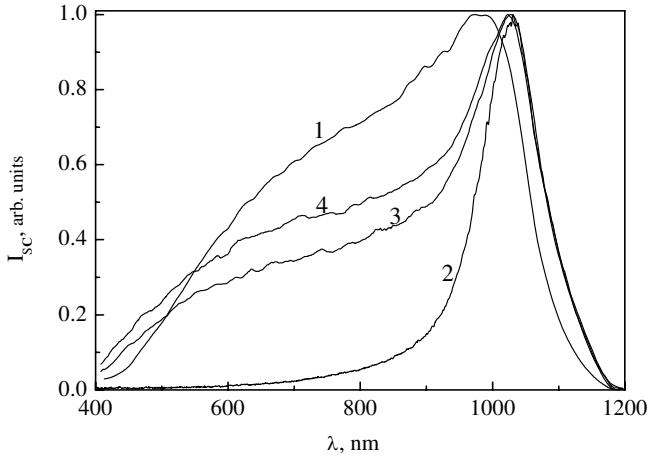

Fig. 8. Spectral dependences of the short-circuit current $I_{\rm SC}$ normalized to the maximum value obtained at low injection levels ($\Delta p \ll n_0$) for the BSC SC samples with isotype $n^+ - n$ (curve *1*) and floating $p^+ - n$ (curves *2, 3, 4*) junctions on the front surface. The irradiance of the stationary illumination of the BSC SC surface $P_{L0} = 0$ (*1, 2*), 6.0 (*3*), and 13.5 (*4*) W/m^2

junction are larger as compared with BSC SCs with an isotype $n^+ - n$ junction.

Figure 7 shows the quantities $V_{\rm OC}$, $I_{\rm SC}$, and $P^* = I_{\rm SC} \times V_{\rm OC}$ as functions of M obtained for the same samples as in Fig. 6. One can see that, with decrease in M, the BSC SC sample with a floating $p^+ - n$ junction manifests a more abrupt reduction of the short-circuit current, open-circuit voltage, and output electric power as compared with the sample with an isotype $n^+ - n$ junction. According to the results of the performed theoretical analysis [formulas (7), (8), and Fig. 4], regularities of this kind should be expected in the case of BSC SCs with a floating $p^+ - n$ junction, where the dominant recombination mechanism at low irradiances of the front surface is the SCR recombination, while this recombination mechanism is absent in BSC SCs with an isotype $n^+ - n$ junction.

The importance of a contribution made to the generalized effective surface recombination velocity on the front BSC SC surface by the recombination in the SCR of a floating $p^+ - n$ junction at low injection levels is also confirmed by the measurements of the spectral dependences of the short-circuit current for the samples with isotype and floating junctions given in Fig. 8. Indeed, the dependences $I_{\rm SC}(\lambda)$ in these two cases measured at low irradiances considerably differ (curves *1* and *2*), whereas the presence of a sharp maximum in the long-wavelength region of the BSC SC with a floating $p^+ - n$ junction (curve *2*) testifies to the high ($> 10^4$ cm/s) effective sur-

face recombination velocity on its front surface. If the dominant recombination mechanism responsible for surface recombination losses on the front surface of such a BSC SC is the recombination in the SCR of a floating $p^+ - n$ junction, then (according to the results of the previous section) its velocity must decrease by many orders of magnitude with increase in the level of injection of nonequilibrium electron pairs in the near-surface region. Moreover, the form of the spectral dependences of the internal quantum efficiency also must essentially change in the way shown in Fig. 3. Indeed, the stationary illumination of the front BSC SC surface by low-intensity white light in the process of measuring the spectral dependences of the short-circuit current resulted in a substantial increase of the internal quantum efficiency in the region $\lambda \leq 900$ nm (curves *3* and *4* in Fig. 8) caused by a considerable decrease of the effective surface recombination velocity on this surface. At the same time, the shape of the spectral characteristic $I_{\rm SC}(\lambda)$ in the BSC SC with an isotype $n^+ - n$ junction (curve *1* in Fig. 8) that is typical of samples with relatively low recombination losses of nonequilibrium electron-hole pairs via surface recombination-active centers is not changed due to a stationary illumination of the front surface. It is worth noting that small values of the quantum efficiency Q in the region $\lambda \leq 600$ nm testify to the presence of the Auger recombination in highly doped p^+ and n^+ regions of solar cells of both types, which requires the optimization when developing high-efficiency silicon-based BSC SCs.

4. Conclusions

The results of theoretical and experimental investigations demonstrate that the use of floating $p^+ - n$ or $n^+ - p$ junctions as antirecombination barriers on the illuminated surface of silicon back side contact solar cells is effective only under the condition of their operation at sufficiently high injection levels of nonequilibrium electron-hole pairs, where the energy band bendings in the floating junction considerably decrease under the action of light. At low injection levels, the recombination velocity in the space-charge region of a floating junction in such cells abruptly increases, which results in a significant reduction of the short-circuit current and the open-circuit voltage as compared with solar cells, in which surface recombination losses on the illuminated surface are minimized due to the formation of an isotype $p^+ - p$ or $n^+ - n$ junction. That is why the use of floating $p^+ - n$ or $n^+ - p$ junctions as antirecombination barriers in silicon photoelectric devices (solar cells, photodetectors, and photosensors) operating at low irradiances of the photodetecting surface is inappropriate.

1. D. De Ceuster, P. Cousins, D. Rose, D. Visente, P. Tipones, and W. Mulligan, in *Proceed. of the 23th European Photovoltaic Solar Energy Conference* (Milan, 2007), p. 816.
2. A.P. Gorban, V.P. Kostylyov, A.V. Sachenko, A.A. Serba, and I.O. Sokolovskyi, Ukr. J. Phys. **51**, 598 (2006).
3. M.I. Yernaux, C. Battochio, P. Verlinden, and F. Van De Wiele, Solar Sells **13**, 83 (1984).
4. W.P. Mulligan, D.H. Rose, M.J. Cudzinovic, D.M. De Ceuster, K.R. McIntosh, D.D. Smith, and R.M. Swanson, in *Proceed. of the 19th European Photovoltaic Solar Energy Conference* (Paris, 2004), p. 387.
5. J. Dicker, J.O. Schumacher, S.W. Glunz, and W. Warta, in *Proceed. of the 2nd World Conference on Photovoltaic Solar Energy Conversion* (Vienna, 1998), p. 95.
6. Nagashima, K. Hokoi, K. Okumura, and M. Yamaguchi, in *Proceed. of the 20th European Photovoltaic Solar Energy Conference* (Barselona, 2005), p.163.
7. A.V. Sachenko, A.P. Gorban, V.P. Kostylyov, and I.O. Sokolovskyi, Fiz. Tekhn. Polupr. **40**, 913 (2006).

Received 02.02.10
Translated from Ukrainian by H.G. Kalyuzhna

ВПЛИВ ПЛАВАЮЧИХ $p - n$ ПЕРЕХОДІВ НА ЕФЕКТИВНІСТЬ КРЕМНІЄВИХ СОНЯЧНИХ ЕЛЕМЕНТІВ ІЗ ТИЛОВИМИ КОНТАКТАМИ

А.П. Горбань, В.П. Костильов, А.В. Саченко, О.А. Серба, І.О. Соколовський, В.В. Черненко

Р е з ю м е

Проведено теоретичний аналіз та експериментальні дослідження характеристик кремнієвих сонячних елементів із тиловою металізацією (СЕТМ) в умовах низької освітленості при наявності плаваючого $p^+ - n$-переходу на фронтальній поверхні. Встановлено, що у даних умовах величини струму короткого замикання та напруги розімкненого кола, а також внутрішній квантовий вихід фотоструму можуть істотно зменшуватись завдяки впливу рекомбінації у приповерхневій області просторового заряду (ОПЗ). Досліджено межі зміни енергетичної освітленості, в яких вказане зменшення достатньо суттєве. Показано, зокрема, що для напруги розімкненого кола $V_{\rm OC}$ діапазон енергетичної освітленості, в якому відбувається зменшення $V_{\rm OC}$, значно ширший, ніж для струму короткого замикання $J_{\rm SC}$. Експериментальні результати узгоджуються з виконаними розрахунками. З отриманих результатів зроблено висновок про те, що плаваючі $p^+ - n$-переходи на фронтальній поверхні кремнієвих СЕТМ доцільно використовувати лише за умови, коли енергетична освітленість становить $\geq$1000 Вт/м^2.